Tailwater level effects on flow conditions at an abrupt drop

Effet de la hauteur d'eau avale sur le ressaut hydraulique au dessus d'une marche

MICHELE MOSSA, *Professor, PhD, MIAHR, Department of Civil and Environmental Engineering, Water Engineering Division, Polytechnic University of Bari, Via E. Orabona, 4 – 70125 Bari, Italy*

ANTONIO PETRILLO, *Professor, Department of Civil and Environmental Engineering, Water Engineering Division, Polytechnic University of Bari, Via E. Orabona, 4 – 70125 Bari, Italy*

HUBERT CHANSON, *Reader, PhD, Eur.Ing., MIEAust., MIAHR , Department of Civil Engineering, The University of Queensland, Brisbane QLD 4072, Australia*

ABSTRACT

This paper presents an experimental study of the transition from supercritical to subcritical flow at an abrupt drop. The paper reports a wide range of experimental conditions and the relevant regime charts. Long-term experimental results show that some flow configurations tend to behave quasi-periodically (i.e. oscillating flow patterns). The experimental results have direct implications on the design and construction of spillway stilling basins where abrupt drops may be used to stabilise the position of the jump. The present study proposes design guidelines taking into account the different flow types, for a range of tailwater flow conditions. These guidelines are essential for a safe and proper operation of stilling basins with abrupt drop.

RÉSUMÉ

On présente une expérimentale de la transition entre un écoulement super-critique et sous-critique à une marche. Cette étude systématique est décrite en détail, avec des abaques de régimes d'écoulement. On montre que le comportement, à long terme, peut être instationnaire et périodique (c.a.d. écoulement oscillatoire). Les résultats expérimentaux ont une implication directe sur la conception et le design de structures de dissipation d'énergie, quand une marche est utilisée pour stabiliser le ressaut hydraulique. On propose des recommandations pratiques pour un fonctionnement sûr de telles structures.

Introduction

A stilling basin is designed to dissipate the kinetic energy of the flow in a hydraulic jump. Sometimes an abrupt drop is introduced to prevent tailwater effects and to stabilise the jump location. The transition from supercritical to subcritical flow at an abrupt drop affects the design and construction of the stilling basins (e.g. Moore and Morgan 1959; Hager and Kawagoshi 1990; Ohtsu and Yasuda 1991; Chanson and Toombes 1998). One objective of the designer is to ensure that the jump is not swept away out of the basin. The design process involves the determination of optimum basin invert elevation, required tailwater elevation, adequate basin length, and desired blocks and end sills.

At an abrupt drop the transition from supercritical to subcritical flow is characterised by several flow patterns depending upon the inflow and tailwater flow conditions. Figure 1 summarises well-acknowledged flow patterns : (1) the A-jump, (2) the wave jump or W-jump, (3) the wave train, (4) the B-jump (or maximum plunging condition) characterised by a plunging jet mechanisms and (5) the minimum B-jump (or limited jump) with a limited hydraulic jump (e.g. Ohtsu and Yasuda 1991). The characteristics of wave jump and wave train are essentially the same (Figs. 1.2 and 1.3) and hereafter the wave jump and wave train will simply be referred to as 'Wave'.

The literature on stilling basin design with abrupt drop provides contradictory advices. Sharp (1974) advised to inhibit the formation of wave jumps (Fig. 1.2) while Armenio et al. (1997) recommend their formation (see also Armenio et al. 2000). The writers believe that the apparently opposing conclusions placed more emphasis on different design optima. Specifically the suggestion of Sharp (1974) yields a stilling basin design with a greater slab thickness to sustain greater pressure fluctuations at the bottom, while the work of Armenio et al. (1997) implies a stilling basin design with higher sidewalls because of the wave formation and smaller floor thickness as a result of smaller pressure fluctuations. The design of stilling basins downstream of gates and control structures must take into consideration the variations of upstream flow conditions (e.g. gate opening, flow rate) and tailwater conditions. Some researchers pointed out the existence of oscillating phenomena, and particularly of cyclic variation of jump types over long period experiments under some flow conditions (e.g. Nebbia 1942; Hager and Bretz 1986; Ohtsu and Yasuda 1991; Abdel Ghafar et al. 1995; Mossa and Petrillo 1997; Mossa and Tolve 1998; Mossa 1999).

The general definition of oscillating characteristics of hydraulic jumps is referred to as a macroscopically visible feature of a hydraulic jump (Mossa 1999). These oscillating characteristics can be: *a)* changes of the different types of hydraulic jumps (variation from one type to another); *b)* horizontal movements of the jump toe (Long et al. 1991); *c)* variations of the velocity components and pressure in the region close the jump roller; *d)* process of formation, development and coalescence of the large scale flow structures. In the present paper the oscillating characteristics are referred to *a)*.

Revision received May 16, 2002. Open for discussion till June 30, 2003.

Although the first writers highlighted such long-duration variations of the flow patterns, the literature is yet unclear on the conditions leading to oscillating jumps and cyclic behaviours. For example, Moore and Morgan (1959) presented diagrams on the flow patterns as a function of Froude number and dimensionless downstream depth, highlighting some doubts about the existence of the wave- and B- jumps, and these graphs did not mention oscillating characteristics. The writers believe that the uncertainty associated with the formation of different types of hydraulic jumps (e.g. stable B type and stable wave jump) derives from long-term fluctuations of the jump flow pattern.

It is the purpose of this paper to assess critically the basic flow patterns for the transition from super- to subcritical flows at an abrupt drop, to present new analysis and experimental results, and to propose new compelling conclusions regarding the changes of the different types of hydraulic jumps and the variation from one type to another.

Experimental set-up and flow conditions

Experimental investigations were carried out in the hydraulic laboratory of the Mediterranean Agronomic Institute (hereafter referred to as IAM) in Valenzano (Bari) in a 7.72-m long 0.3-m wide rectangular channel with sidewall height of 0.40 m, and in the laboratory of the Civil and Environmental Engineering Department – Water Engineering Division (hereafter referred to as SIA) of Bari Polytechnic University in a 0.40-m wide 24.4-m long channel (0.5 m sidewall height). The walls and bottoms of both channels were made of Plexiglas. In the IAM channel, the step was built of polished and varnished wooden boards and the step was located 0.79-m downstream of the upstream gate. The height of the abrupt drop (s) was 5.30, 10.00 and 16.00 cm. In the SIA channel, the abrupt drop was made of Plexiglas and located 0.8-m downstream of the gate. The abrupt drop height s was equal to 3.20 and 6.52 cm.

Discharges were measured with a triangular sharp-crested weir. Measurements of the upstream and downstream water depths were carried out with electric hydrometers type point gauge supplied with electronic integrators which allowed the estimate of the time-averaged flow depth. The hydrometers are supplied with verniers allowing measurement accuracy of ±0.1 mm. Water discharge and hydrodynamic conditions were regulated by two gates placed at the upstream and downstream ends of the channels.

For some runs, pressure measurements under the jumps were obtained using a pressure transducer type 4310 of Society TransInstruments with relative difference pressure range equal to 0÷7500 Pa. The pressure tap was connected to the transducer using a rigid tube with 2 mm diameter and 0.4 m of length. Amplifier and conditioner were used to adjust the signal output of the transducer for resolution and acceptable range of the A/D board.

In addition, a videocamera was used to film the jump for some runs.

Measurement technique

For each experiment, measurements were carried out after waiting a minimum of one hour after the establishment of the flow. Afterwards the measurements were conducted for periods of no less than one hour and up to 2 hours. Table 1 summarises the experimental flow conditions, where y_1 is the inflow water depth, y_t is the water depth downstream of jump, F_1 is the inflow Froude number, and Re is the Reynolds number defined as $Re=V_1y_1/\nu=V_ty_t/\nu$, where V_1 and V_t are the flow velocities at water depths y_1 and y_t, respectively, and ν the kinematic water viscosity at the run temperature (Fig. 1). The upstream flow depth y_1 was measured where the jump toe was positioned on the average for A- and limited jumps, and at the step brink for the cases of maximum plunging condition, wave jumps and wave trains. Figure 1 shows the locations where y_1 and y_t were measured for each flow pattern. In Table 1, column 1, the runs denoted types B and V refer to the SIA and IAM channels respectively.

Basic flow patterns

The flow pattern was carefully analysed for each run and the result is reported in Table 1, column 2. These are the A-jump, the Wave flow (wave jump or wave train), maximum plunging condition (also referred to as B-jump with plunging jet mechanism) and limited jump (also referred to as minimum B-jump with limited hydraulic jump).

For some flow conditions, oscillatory flow patterns were observed during long-duration tests. For example, the flow would appear to be an A-jump, then become a Wave flow and later be again an A-jump (A-wave flow pattern). Two oscillatory flow patterns were observed: the B-wave (oscillatory flow patterns between B-jump and Wave jump/train; an example is shown in Figs. 2a-2f, where six snapshots of the film were chosen for configuration B61 of Table 1) and the A-wave (oscillatory flow patterns between A-jump and Wave jump/train). Experimental observations are highlighted in Table 1, column 2.

Such oscillating characteristics of hydraulics jumps were previously observed. Nebbia (1942) showed that '*in the scour processes taking place downstream of spillways, the flow often transforms into two different types which follow one another with quasi-periodic oscillation. The shift from one type to another may be sudden or gradual, due to causes which are still unknown, through a swift following of instantaneous transition profiles*'. He indicated that these phenomena were described by Roth during the flooding of the Sihl in Zurich, as well as by Gruner and Locker, who observed them in the laboratory. Other authors (Hager and Bretz 1986; Ohtsu and Yasuda 1991) pointed out the existence of oscillations between jump types.

Theoretical background

The momentum equation written between the upstream section (subscript *1*) and the downstream section (subscript *t*) yields :

$$(\gamma/g)q(V_t - V_1) = P_s + P_1 - P_t \qquad (1)$$

where γ is the specific weight of water, g is the gravity acceleration, q is the discharge per unit width, P_1 and P_t are total pressure

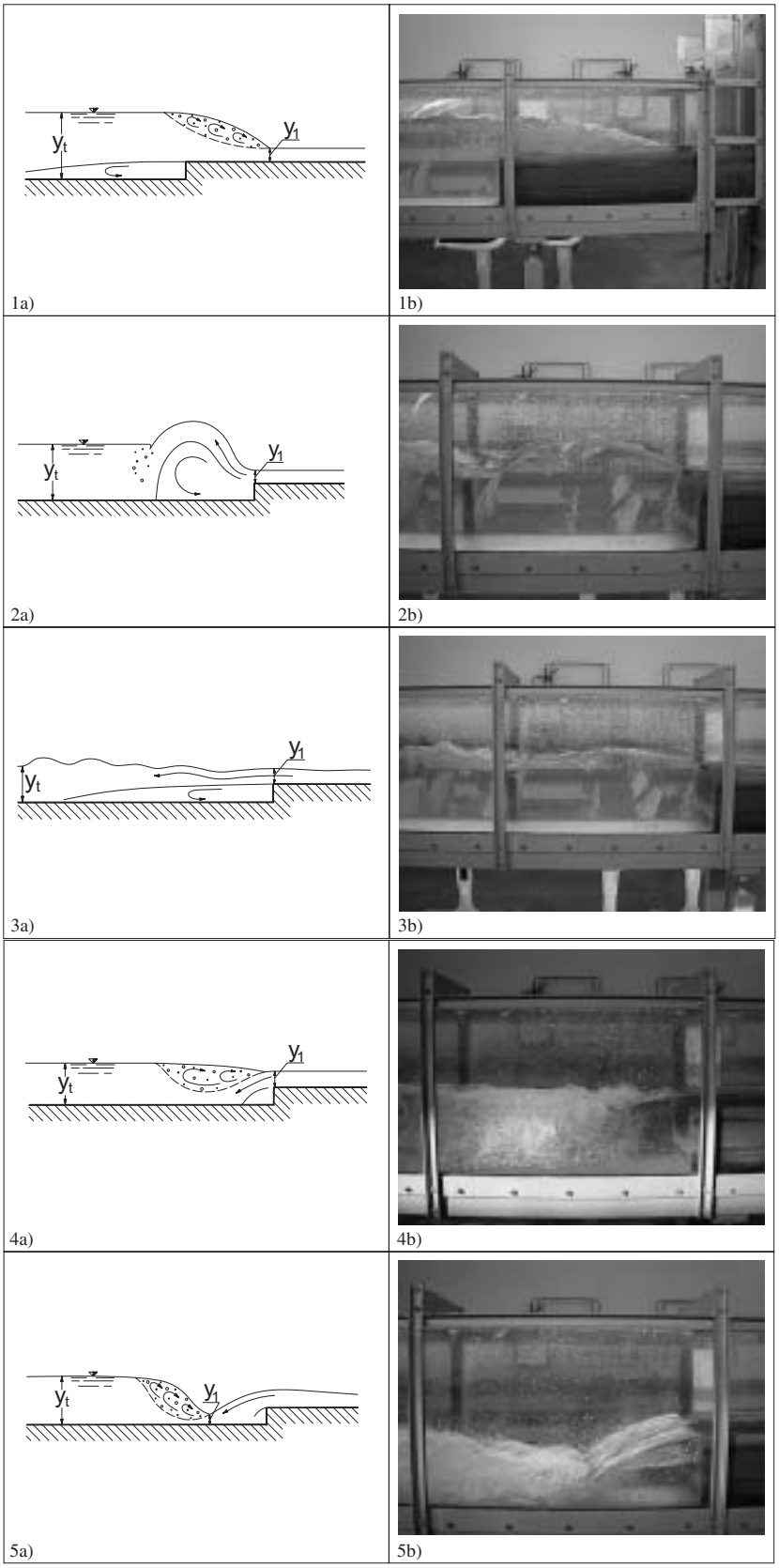

Fig. 1 Flow conditions. From the top: (1a-b) A-jump; (2a-b) wave jump; (3a-b) wave train; (4a-b) B-jump (maximum plunging condition); (5a-b) minimum B-jump (limited jump).

forces per unit width at sections 1 and t, and P_s is the total pressure force per unit width on the vertical face of the drop (e.g. Ohtsu and Yasuda 1991) (Fig. 3). For some configurations these terms may be transformed as

$$P_1 = \gamma\, y_1^2/2; \quad P_t = \gamma\, y_t^2/2; \quad P_s = k\gamma s\left(y_1 + s/2\right) \tag{2}$$

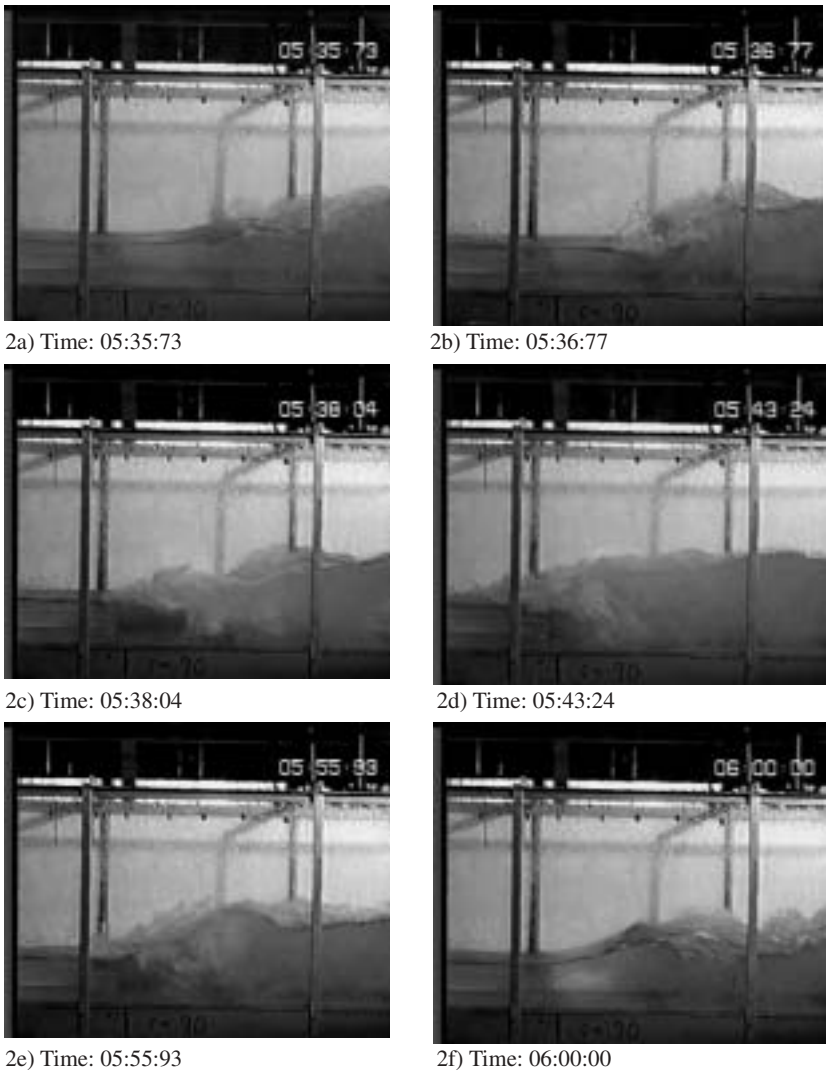

2a) Time: 05:35:73 2b) Time: 05:36:77

2c) Time: 05:38:04 2d) Time: 05:43:24

2e) Time: 05:55:93 2f) Time: 06:00:00

Fig. 2 Oscillatory flow patterns between B-jump and Wave jump (configuration B61 of Table 1); time is expressed in minutes, seconds and hundredths of seconds from the shooting start.

Table 1 Main parameters of the investigated flow configurations

Run	Flow type	y_1	y_t	V_1	V_t	F_1	y_t/y_1	Re	s	s/y_1
		cm	cm	m/s	m/s				cm	
(1)	(2)	(3)	(4)	(5)	(6)	(7)	(8)	(9)	(10)	(11)
B1	Limited jump	1.45	9.82	2.45	0.36	6.51	6.77	3.20E+04	3.2	2.2
B2	Limited jump	1.42	11.59	2.51	0.31	6.71	8.16	3.20E+04	3.2	2.3
B3	Limited jump	1.41	12.34	2.58	0.29	6.93	8.75	3.30E+04	3.2	2.3
B4	Max.plung.condit.	1.08	13.35	3.36	0.27	10.33	12.36	3.30E+04	3.2	3.0
B5	Max.plung.condit.	1.06	13.91	3.30	0.25	10.25	13.12	3.20E+04	3.2	3.0
B6	Max.plung.condit.	1.09	14.39	3.21	0.24	9.83	13.2	3.20E+04	3.2	2.9
B7	**B-wave**	1.09	14.52	3.09	0.23	9.44	13.32	3.10E+04	3.2	2.9
B8	Wave	1.09	14.68	3.11	0.23	9.52	13.47	3.10E+04	3.2	2.9
B9	Wave	1.08	14.95	3.24	0.23	9.96	13.84	3.20E+04	3.2	3.0
B10	Wave	1.08	15.31	3.24	0.23	9.96	14.18	3.20E+04	3.2	3.0
B11	Wave	1.07	15.64	3.27	0.22	10.10	14.62	3.20E+04	3.2	3.0
B12	A-jump	1.06	15.75	3.20	0.22	9.92	14.86	3.10E+04	3.2	3.0

B13	A-jump	1.08	16.09	3.14	0.21	9.65	14.90	3.10E+04	3.2	3.0
B14	A-jump	1.05	16.56	3.23	0.20	10.07	15.77	3.10E+04	3.2	3.1
B15	A-jump	1.07	16.6	3.17	0.20	9.79	15.51	3.10E+04	3.2	3.0
B16	Limited jump	1.75	15.38	2.86	0.33	6.90	8.79	4.60E+04	3.2	1.8
B17	Max.plung.condit.	1.81	15.98	2.76	0.31	6.56	8.83	4.60E+04	3.2	1.8
B18	Max.plung.condit.	1.78	16.46	2.81	0.30	6.73	9.25	4.60E+04	3.2	1.8
B19	Max.plung.condit.	1.73	17.1	2.89	0.29	7.02	9.88	4.60E+04	3.2	1.9
B20	Wave	1.75	17.44	2.83	0.28	6.83	9.97	4.50E+04	3.2	1.8
B21	Wave	1.69	17.67	2.93	0.28	7.20	10.46	4.50E+04	3.2	1.9
B22	Wave	1.82	17.94	2.72	0.28	6.44	9.86	4.50E+04	3.2	1.8
B23	A-jump	1.7	18.14	2.91	0.27	7.14	10.67	4.50E+04	3.2	1.9
B24	A-jump	1.7	18.26	2.80	0.26	6.86	10.74	4.30E+04	3.2	1.9
B25	A-jump	1.67	18.88	2.85	0.25	7.05	11.31	4.30E+04	3.2	1.9
B26	Limited jump	4.23	15.08	1.60	0.45	2.48	3.57	6.10E+04	3.2	0.8
B27	Limited jump	5.27	15.22	1.28	0.44	1.78	2.89	6.10E+04	3.2	0.6
B28	Max.plung.condit.	3.78	16.1	1.79	0.42	2.94	4.26	6.10E+04	3.2	0.9
B29	Max.plung.condit.	3.85	16.3	1.70	0.40	2.77	4.23	5.70E+04	3.2	0.8
B30	Max.plung.condit.	3.39	16.78	2.02	0.41	3.50	4.95	6.00E+04	3.2	0.9
B31	Max.plung.condit.	3.5	16.37	1.93	0.41	3.29	4.68	6.10E+04	3.2	0.9
B32	**B-wave**	3.5	16.63	1.93	0.41	3.29	4.75	6.10E+04	3.2	0.9
B33	Wave	3.41	17.38	2.01	0.39	3.47	5.10	6.00E+04	3.2	0.9
B34	Wave	3.35	17.21	1.94	0.38	3.38	5.14	5.90E+04	3.2	1.0
B35	Wave	3.6	16.98	1.87	0.40	3.14	4.72	5.80E+04	3.2	0.9
B36	Wave	3.6	17.58	1.80	0.37	3.04	4.88	5.90E+04	3.2	0.9
B37	**A-wave**	3.71	17.65	1.81	0.38	3.00	4.76	5.80E+04	3.2	0.9
B38	**A-wave**	3.48	18.18	1.87	0.36	3.20	5.22	5.90E+04	3.2	0.9
B39	A-jump	3.14	17.97	2.09	0.36	3.76	5.72	5.70E+04	3.2	1.0
B40	A-jump	3.19	18.2	2.04	0.36	3.64	5.71	5.90E+04	3.2	1.0
B41	A-jump	3.12	18.63	2.08	0.35	3.76	5.97	5.90E+04	3.2	1.0
B42	Limited jump	2.11	13.09	2.23	0.36	4.89	6.20	4.00E+04	6.52	3.1
B43	Limited jump	2.68	13.54	1.75	0.35	3.42	5.05	4.00E+04	6.52	2.4
B44	Max.plung.condit.	1.88	15.09	2.50	0.31	5.82	8.03	4.00E+04	6.52	3.5
B45	Max.plung.condit.	1.88	15.31	2.50	0.31	5.82	8.14	4.00E+04	6.52	3.5
B46	Max.plung.condit.	1.78	15.94	2.67	0.30	6.39	8.96	4.00E+04	6.52	3.7
B47	Max.plung.condit.	1.94	16.2	2.45	0.29	5.61	8.35	4.00E+04	6.52	3.4
B48	**B-wave**	1.94	17.07	2.45	0.28	5.61	8.80	4.00E+04	6.52	3.4
B49	Wave	1.93	17.49	2.46	0.27	5.66	9.06	4.00E+04	6.52	3.4
B50	Wave	1.97	18.16	2.41	0.26	5.48	9.22	4.10E+04	6.52	3.3
B51	Wave	2.02	18.83	2.35	0.25	5.28	9.32	4.10E+04	6.52	3.2
B52	Wave	2.02	19.33	2.36	0.25	5.30	9.57	4.10E+04	6.52	3.2
B53	A-jump	1.89	19.78	2.52	0.24	5.86	10.47	4.10E+04	6.52	3.5
B54	A-jump	1.97	20.6	2.42	0.23	5.51	10.46	4.10E+04	6.52	3.3
B55	Limited jump	4.21	16.74	1.89	0.47	2.94	3.98	6.80E+04	6.52	1.6
B56	Limited jump	3.41	17.9	2.33	0.44	4.03	5.25	6.80E+04	6.52	1.9
B57	Limited jump	3.92	18.78	2.05	0.43	3.30	4.79	6.70E+04	6.52	1.7
B58	Max.plung.condit.	3.4	20.03	2.36	0.40	4.09	5.89	6.70E+04	6.52	1.9
B59	Max.plung.condit.	3.43	20.37	2.34	0.39	4.04	5.94	6.70E+04	6.52	1.9
B60	Max.plung.condit.	3.01	20.4	2.67	0.39	4.91	6.78	6.70E+04	6.52	2.2
B61	**B-wave**	3.13	22.34	2.35	0.33	4.25	7.14	6.20E+04	6.52	2.1

B62	Wave	3.02	23.69	2.66	0.34	4.89	7.84	6.70E+04	6.52	2.2
B63	Wave	3.09	24.14	2.60	0.33	4.72	7.81	6.70E+04	6.52	2.1
B64	A-jump	2.93	25.13	2.74	0.32	5.11	8.58	6.80E+04	6.52	2.2
B65	A-jump	3.5	25.86	2.28	0.31	3.89	7.39	6.60E+04	6.52	1.9
B66	Limited jump	3.13	17.13	2.34	0.43	4.22	5.47	6.00E+04	6.52	2.1
B67	Limited jump	4.55	18.15	1.61	0.40	2.41	3.99	5.90E+04	6.52	1.4
B68	Max.plung.condit.	2.49	18.78	2.94	0.39	5.95	7.54	5.90E+04	6.52	2.6
B69	Max.plung.condit.	2.56	19.42	2.84	0.37	5.66	7.59	5.90E+04	6.52	2.6
B70	Max.plung.condit.	2.36	20.52	3.08	0.35	6.40	8.69	5.90E+04	6.52	2.8
B71	Max.plung.condit.	2.4	21.54	3.03	0.34	6.24	8.98	5.90E+04	6.52	2.7
B72	**B-wave**	2.47	22.2	2.95	0.33	5.99	8.99	5.90E+04	6.52	2.6
B73	Wave	2.43	22.27	2.99	0.33	6.12	9.16	5.90E+04	6.52	2.7
B74	Wave	2.45	22.84	2.95	0.32	6.02	9.32	5.80E+04	6.52	2.7
B75	Wave	2.44	23.73	2.96	0.30	6.06	9.73	5.90E+04	6.52	2.7
B76	**A-wave**	2.42	24.33	2.99	0.30	6.13	10.05	5.90E+04	6.52	2.7
B77	A-jump	2.32	25.23	3.12	0.29	6.53	10.88	5.90E+04	6.52	2.8
V1	Limited jump	3.61	13.21	1.48	0.40	2.49	3.66	4.10E+04	5.3	1.5
V2	Limited jump	2.87	14.82	1.86	0.36	3.51	5.16	4.10E+04	5.3	1.9
V3	Max.plung.condit.	2.51	15.3	2.13	0.35	4.29	6.10	4.10E+04	5.3	2.1
V4	Max.plung.condit.	2.46	16.21	2.17	0.33	4.42	6.59	4.10E+04	5.3	2.2
V5	Max.plung.condit.	2.43	16.8	2.20	0.32	4.50	6.91	4.10E+04	5.3	2.2
V6	**B-wave**	2.52	17.92	2.09	0.29	4.20	7.11	4.50E+04	5.3	2.1
V7	Wave	2.64	18.19	2.02	0.29	3.96	6.89	4.10E+04	5.3	2.0
V8	Wave	2.73	18.79	1.95	0.28	3.77	6.88	4.10E+04	5.3	1.9
V9	Wave	2.66	19.12	2.00	0.28	3.92	7.19	4.10E+04	5.3	2.0
V10	Wave	2.74	19.67	1.94	0.27	3.75	7.18	4.10E+04	5.3	1.9
V11	A-jump	2.36	20.13	2.26	0.26	4.69	8.53	4.10E+04	5.3	2.3
V12	A-jump	2.51	20.58	2.12	0.26	4.28	8.20	4.10E+04	5.3	2.1
V13	A-jump	2.93	20.8	1.82	0.26	3.39	7.10	4.10E+04	5.3	1.8
V14	A-jump	3.2	21.18	1.66	0.25	2.97	6.62	4.10E+04	5.3	1.7
V15	Limited jump	2.14	12.27	2.22	0.39	4.83	5.73	3.70E+04	5.3	2.5
V16	Limited jump	2.61	13.89	1.82	0.34	3.59	5.32	3.70E+04	5.3	2.0
V17	Max.plung.condit.	1.79	14.39	2.65	0.33	6.32	8.04	3.70E+04	5.3	3.0
V18	Max.plung.condit.	1.8	15.34	2.63	0.31	6.27	8.52	3.70E+04	5.3	2.9
V19	Max.plung.condit.	1.88	15.74	2.52	0.30	5.87	8.37	3.70E+04	5.3	2.8
V20	**B-wave**	1.91	17.5	2.47	0.27	5.72	9.16	3.90E+04	5.3	2.8
V21	Wave	1.88	17.89	2.52	0.26	5.87	9.52	3.70E+04	5.3	2.8
V22	Wave	1.94	18.34	2.44	0.26	5.60	9.45	3.70E+04	5.3	2.7
V23	Wave	1.96	18.78	2.42	0.25	5.52	9.58	3.70E+04	5.3	2.7
V24	Wave	1.95	19.3	2.43	0.25	5.56	9.90	3.70E+04	5.3	2.7
V25	A-jump	1.85	19.59	2.56	0.24	6.02	10.59	3.70E+04	5.3	2.9
V26	A-jump	1.75	19.99	2.71	0.24	6.54	11.42	3.70E+04	5.3	3.0
V27	A-jump	1.94	20.55	2.44	0.23	5.60	10.59	3.70E+04	5.3	2.7
V28	Limited jump	3.49	13.17	1.77	0.47	3.03	3.77	5.00E+04	5.3	1.5
V29	Limited jump	3.08	13.84	2.01	0.45	3.66	4.49	5.00E+04	5.3	1.7
V30	Max.plung.condit.	3.28	14.71	1.89	0.42	3.33	4.48	5.00E+04	5.3	1.6
V31	Max.plung.condit.	3.3	15.11	1.88	0.41	3.30	4.58	5.00E+04	5.3	1.6
V32	Max.plung.condit.	3.31	15.55	1.87	0.40	3.28	4.70	5.00E+04	5.3	1.6
V33	**B-wave**	3.47	16.37	1.78	0.38	3.06	4.72	5.10E+04	5.3	1.5

V34	Wave	3.38	16.51	1.83	0.38	3.18	4.88	5.00E+04	5.3	1.6
V35	Wave	3.45	16.99	1.79	0.36	3.08	4.92	5.00E+04	5.3	1.5
V36	Wave	3.58	17.67	1.73	0.35	2.92	4.94	5.00E+04	5.3	1.5
V37	Wave	3.72	18.11	1.66	0.34	2.76	4.87	5.00E+04	5.3	1.4
V38	A-jump	3.25	18.71	1.91	0.33	3.37	5.76	5.00E+04	5.3	1.6
V39	A-jump	3.11	19.22	1.99	0.32	3.60	6.18	5.00E+04	5.3	1.7
V40	A-jump	3.1	19.55	2.00	0.32	3.62	6.31	5.00E+04	5.3	1.7
V41	Limited jump	1.78	7.16	1.41	0.35	3.38	4.02	1.90E+04	5.3	3.0
V42	Limited jump	1.37	8.99	1.83	0.28	5.00	6.56	1.90E+04	5.3	3.9
V43	Limited jump	2.15	9.61	1.17	0.26	2.54	4.47	1.90E+04	5.3	2.5
V44	Max.plung.condit.	1.01	10.03	2.49	0.25	7.90	9.93	1.90E+04	5.3	5.3
V45	Max.plung.condit.	1	10.41	2.51	0.24	8.02	10.41	1.90E+04	5.3	5.3
V46	Max.plung.condit.	1.01	10.95	2.49	0.23	7.90	10.84	1.90E+04	5.3	5.3
V47	**B-wave**	1	12.08	2.51	0.21	8.02	12.08	1.90E+04	5.3	5.3
V48	Wave	0.99	13.39	2.54	0.19	8.14	13.53	1.90E+04	5.3	5.4
V49	Wave	1	13.78	2.51	0.18	8.02	13.78	1.90E+04	5.3	5.3
V50	Wave	1.01	14.32	2.49	0.18	7.90	14.18	1.90E+04	5.3	5.3
V51	A-jump	0.89	15.33	2.64	0.15	8.93	17.22	1.80E+04	5.3	6.0
V52	A-jump	0.82	15.87	2.86	0.15	10.09	19.35	1.80E+04	5.3	6.5
V53	A-jump	0.81	16.26	2.90	0.14	10.28	20.07	1.80E+04	5.3	6.5
V54	Limited jump	3.37	13.07	1.57	0.40	2.73	3.88	4.50E+04	10	3.0
V55	Limited jump	3.27	14.26	1.62	0.37	2.85	4.36	4.50E+04	10	3.1
V56	Max.plung.condit.	2.41	15.25	2.19	0.35	4.51	6.33	4.50E+04	10	4.2
V57	Max.plung.condit.	2.45	16.13	2.16	0.33	4.40	6.58	4.50E+04	10	4.1
V58	Max.plung.condit.	2.46	17.17	2.15	0.31	4.37	6.98	4.50E+04	10	4.1
V59	**B-wave**	2.58	19.56	2.12	0.28	4.21	7.58	4.90E+04	10	3.9
V60	Wave	2.54	20.44	2.15	0.27	4.31	8.05	4.90E+04	10	3.9
V61	Wave	2.61	21.55	2.09	0.25	4.13	8.26	4.90E+04	10	3.8
V62	Wave	2.72	22.57	2.01	0.24	3.89	8.30	4.90E+04	10	3.7
V63	Wave	2.76	23.03	1.98	0.24	3.80	8.34	4.90E+04	10	3.6
V64	A-jump	2.41	23.68	2.27	0.23	4.66	9.83	4.90E+04	10	4.2
V65	A-jump	2.45	24.63	2.23	0.22	4.55	10.05	4.90E+04	10	4.1
V66	A-jump	2.4	25.26	2.28	0.22	4.69	10.53	4.90E+04	10	4.2
V67	Limited jump	2.52	12.11	1.80	0.38	3.63	4.81	4.30E+04	10	4.0
V68	Limited jump	2.49	13.69	1.83	0.33	3.69	5.50	4.30E+04	10	4.0
V69	Max.plung.condit.	1.85	15.25	2.46	0.30	5.77	8.24	4.30E+04	10	5.4
V70	Max.plung.condit.	1.84	16.02	2.47	0.28	5.81	8.71	4.30E+04	10	5.4
V71	Max.plung.condit.	1.87	17.06	2.43	0.27	5.67	9.12	4.30E+04	10	5.4
V72	Wave	1.88	19.07	2.42	0.24	5.63	10.14	4.30E+04	10	5.3
V73	Wave	1.9	20.13	2.39	0.23	5.54	10.59	4.30E+04	10	5.3
V74	Wave	1.97	20.92	2.31	0.22	5.25	10.62	4.30E+04	10	5.1
V75	A-jump	1.77	23.11	2.57	0.20	6.16	13.06	4.30E+04	10	5.7
V76	A-jump	1.64	23.7	2.77	0.19	6.91	14.45	4.30E+04	10	6.1
V77	A-jump	1.6	24.2	2.84	0.19	7.17	15.13	4.30E+04	10	6.3
V78	Limited jump	1.73	7.03	1.33	0.33	3.22	4.06	2.10E+04	10	5.8
V79	Limited jump	1.59	8.79	1.44	0.26	3.66	5.53	2.10E+04	10	6.3
V80	Limited jump	1.65	8.85	1.39	0.26	3.46	5.36	2.10E+04	10	6.1
V81	Max.plung.condit.	0.99	10.33	2.32	0.22	7.44	10.43	2.10E+04	10	10.1
V82	Max.plung.condit.	1.01	11.18	2.22	0.20	7.06	11.07	2.10E+04	10	9.9

V83	Max.plung.condit.	1	12.2	2.24	0.18	7.16	12.20	2.10E+04	10	10.0
V84	**B-wave**	1.01	14.32	2.22	0.16	7.06	14.18	2.10E+04	10	9.9
V85	Wave	1.03	15.66	2.18	0.14	6.85	15.20	2.10E+04	10	9.7
V86	Wave	1.04	16.55	2.16	0.14	6.75	15.91	2.10E+04	10	9.6
V87	Wave	1.05	17.66	2.14	0.13	6.66	16.82	2.10E+04	10	9.5
V88	Wave	1.06	17.97	2.12	0.12	6.56	16.95	2.10E+04	10	9.4
V89	A-jump	0.95	18.69	2.36	0.12	7.73	19.67	2.10E+04	10	10.5
V90	A-jump	0.89	19.52	2.52	0.11	8.53	21.93	2.10E+04	10	11.2
V91	A-jump	0.82	20.24	2.74	0.11	9.65	24.68	2.10E+04	10	12.2
V92	Limited Jump	2.31	12.94	2.01	0.36	4.22	5.60	3.90E+04	16	6.9
V93	Limited Jump	3.5	14.01	1.33	0.33	2.26	4.00	3.90E+04	16	4.6
V94	Max.plung.condit.	2.66	19.48	1.74	0.24	3.41	7.32	3.90E+04	16	6.0
V95	Max.plung.condit.	2.66	20.69	1.65	0.21	3.23	7.78	3.50E+04	16	6.0
V96	Wave	2.76	22.16	1.68	0.21	3.23	8.03	3.90E+04	16	5.8
V97	Wave	2.77	22.74	1.58	0.19	3.04	8.21	3.50E+04	16	5.8
V98	A-jump	3.51	26.39	1.25	0.17	2.13	7.52	3.50E+04	16	4.6
V99	A-jump	3.81	26.5	1.15	0.17	1.88	6.96	3.50E+04	16	4.2
V100	Limited jump	1.64	5.96	1.86	0.51	4.63	3.63	2.50E+04	16	9.8
V101	Limited jump	1.05	9.13	2.90	0.33	9.03	8.70	2.50E+04	16	15.2
V102	Limited jump	1.06	10.2	2.87	0.30	8.91	9.62	2.50E+04	16	15.1
V103	Max.plung.condit.	1.01	17.44	3.01	0.17	9.58	17.27	2.50E+04	16	15.8
V104	Max.plung.condit.	1.08	18.01	2.82	0.17	8.66	16.68	2.50E+04	16	14.8
V105	Wave	1.06	18.81	2.87	0.16	8.91	17.75	2.50E+04	16	15.1
V106	Wave	1.08	19.41	2.82	0.16	8.66	17.97	2.50E+04	16	14.8
V107	Wave	1.15	19.69	2.65	0.15	7.88	17.12	2.50E+04	16	13.9
V108	Wave	1.2	20.84	2.54	0.15	7.39	17.37	2.50E+04	16	13.3
V109	A-jump	1.15	21.87	2.65	0.14	7.88	19.02	2.50E+04	16	13.9
V110	A-jump	1.59	23.11	1.91	0.13	4.85	14.53	2.50E+04	16	10.1
V111	A-jump	1.21	23.56	2.52	0.13	7.30	19.47	2.50E+04	16	13.2
V112	Limited Jump	2.17	11.94	1.93	0.35	4.18	5.50	3.40E+04	16	7.4
V113	Limited Jump	2	13.17	2.09	0.32	4.72	6.59	3.40E+04	16	8.0
V114	Max.plung.condit.	1.96	19	2.13	0.22	4.87	9.69	3.40E+04	16	8.2
V115	Max.plung.condit.	1.94	20.39	2.16	0.21	4.94	10.51	3.40E+04	16	8.3
V116	Max.plung.condit.	1.95	21.23	2.14	0.20	4.90	10.89	3.40E+04	16	8.2
V117	Wave	1.87	22.07	2.24	0.19	5.22	11.80	3.40E+04	16	8.6
V118	Wave	1.83	22.7	2.29	0.18	5.39	12.40	3.40E+04	16	8.7
V119	Wave	1.95	23.02	2.14	0.18	4.90	11.81	3.40E+04	16	8.2
V120	Wave	2.05	23.91	2.04	0.17	4.55	11.66	3.40E+04	16	7.8
V121	A-jump	1.81	26.06	2.31	0.16	5.48	14.40	3.40E+04	16	8.8
V122	A-jump	2.85	26.43	1.47	0.16	2.78	9.27	3.40E+04	16	5.6
V123	A-jump	1.96	26.98	2.13	0.16	4.87	13.77	3.40E+04	16	8.2
V124	A-jump	1.65	27.59	2.53	0.15	6.30	16.72	3.40E+04	16	9.7
V125	Limited Jump	2.59	12.22	2.47	0.52	4.89	4.72	5.00E+04	16	6.2
V126	Limited Jump	2.26	13.25	2.83	0.48	6.00	5.86	5.00E+04	16	7.1
V127	Max.plung.condit.	2.21	21.43	2.89	0.30	6.21	9.70	5.00E+04	16	7.2
V128	Wave	2.28	23.21	2.80	0.28	5.92	10.18	5.00E+04	16	7.0
V129	Wave	2.3	23.3	2.78	0.27	5.85	10.13	5.00E+04	16	7.0
V130	Wave	2.25	24.16	2.84	0.26	6.04	10.74	5.00E+04	16	7.1
V131	Wave	2.3	24.85	2.78	0.26	5.85	10.80	5.00E+04	16	7.0

V132	A-jump	2.12	26.54	3.01	0.24	6.61	12.52	5.00E+04	16	7.6
V133	A-jump	2.1	27.13	3.04	0.24	6.70	12.92	5.00E+04	16	7.6
V134	A-jump	2.61	27.37	2.45	0.23	4.84	10.49	5.00E+04	16	6.1

Notes: Column 1: BXX = run in SIA channel; VXXX = run in IAM channel.
Column 2: A-jump = A-jump; Wave = wave jump (W-jump) or wave train; Max. plung. condit. = B-jump with plunging jet mechanism; Limited jump = minimum B-jump with limited hydraulic jump; B-wave = oscillatory flow patterns between B-jump and Wave jump/train; A-wave = oscillatory flow patterns between A-jump and Wave jump/train

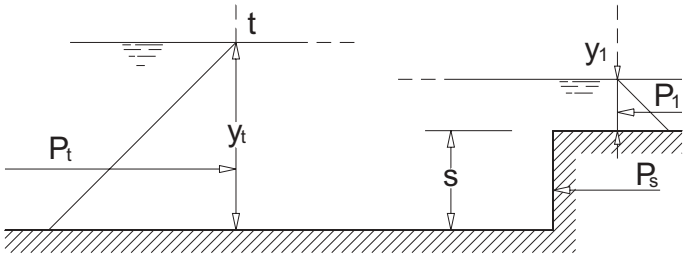

Fig. 3 Definition sketch.

where k is a pressure correction coefficient equal to the ratio of the actual pressure force on the step face to the hydrostatic pressure force. Substituting Eqs. (2) into Eq. (1) the momentum equation becomes

$$F_1^2 = \left\{\left(y_t/y_1\right)^2 - k\left(s/y_1\right)^2 - 2k\left(s/y_1\right) - 1\right\} \Big/ \left\{2\left[1 - 1/\left(y_t/y_1\right)\right]\right\} \qquad (3)$$

where F_1 is the inflow Froude number.

Ohtsu and Yasuda (1991) deduced the pressure correction coefficient k from bottom pressure measurements. In the present study, the inflow Froude number was predicted using the equations proposed by Ohtsu and Yasuda (1991) for wave jumps (with $2.5 \div 3.0 \leq F_1 \leq 5.0$), for maximum plunging conditions (with $1.0 \leq F_1 \leq 5.0$ and $0.5 \div 1.5 \leq s/y_1 \leq 8.0 \div 9.0$, i.e. low drop case) and for A-jump flows (with $0.5 \div 1.5 \leq s/y_1 \leq 8.0 \div 9.0$).

Figure 4 compares the observed values of the inflow Froude number F_1 (present study) as functions of the predictions. The mean experimental absolute error equals ±0.3.

A detailed dimensional analysis indicates that the type of flow pattern may be expressed as:

$$\text{Flow pattern} = f\left(F_1, Re, We, \frac{y_t}{y_1}, \frac{s}{y_1}, \frac{\varepsilon}{y_1}\right) \qquad (4)$$

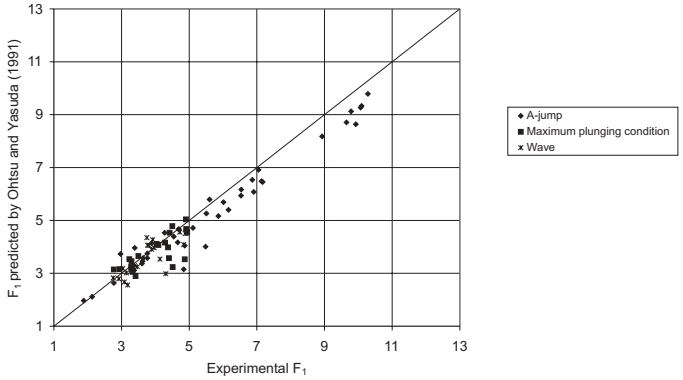

Fig. 4 Comparison between experimental inflow Froude numbers of the present paper and predicted inflow Froude numbers.

where Re is the Reynolds number, We is the Weber number and ε is the channel equivalent roughness height. In the present study, the variability of each dimensionless number was not considered. The experiments were conducted for large Reynolds numbers ranging from 1.8E+4 to 7E+4 and surface tension effects were observed to be negligible. The effects of the channel roughness were ignored because the channel walls were hydraulically smooth. Equation (4) yields

$$\text{Flow pattern} = f\left(F_1, \frac{y_t}{y_1}, \frac{s}{y_1}\right) \qquad (5)$$

Several researchers investigated the effects of the upstream Froude number and tailwater levels on the flow pattern (e.g. Moore and Morgan 1959). In the following paragraphs, the writers will highlight the effects of the dimensionless drop height s/y_1, and of the bottom shape, on the type of flow pattern.

Results

The experimental observations suggest that the relationship between the tailwater depth ratio y_t/y_1 and the upstream Froude number F_1 is a function of the relative step height s/y_1. In order to avoid using a three-dimensional diagram, the relationship between the upstream Froude number F_1 and the tailwater depth ratio y_t/y_1 is presented by subdividing all the flow conditions into groups characterised by a range of variability of the parameter s/y_1. Hsu (1950) produced a correlation using this technique and his results were published in Chow (1959). Rao and Rajaratnam (1963) used a similar technique for their investigation on submerged hydraulic jumps. The present study presents a wider range of variability of the relative step height, including configurations with oscillations between two different flow patterns. The results are presented in the form of eleven different diagrams as functions of the relative step height s/y_1:

s/y_1=0.6-1.1	Fig. 5
s/y_1=1.1-1.6	Fig. 6
s/y_1=1.6-2.1	Fig. 7
s/y_1=2.1-2.6	Fig. 8
s/y_1=2.6-3.1	Fig. 9
s/y_1=3.1-4.1	Fig. 10
s/y_1=4.1-5.1	Fig. 11

s/y_1=5.1-6.1	Fig. 12
s/y_1=6.1-7.1	Fig. 13
s/y_1=7.1-8.1	Fig. 14
s/y_1=8.1-15.8	Fig. 15

Each group is characterised by a range of relative step height s/y_1 for which the relationship between F_1 and y_t/y_1 (i.e., area of validity of each flow) was found to be independent of the relative step height s/y_1. The experimental results show that the groups with relatively small value of s/y_1 are characterised by smaller range of s/y_1. The regime chart of Fig. 15 is an exception, because the experimental results show that the relationship F_1-y_t/y_1 is independent of the relative step height for s/y_1 = 8.1-15.8. In each diagram (Figs. 5 to 15), the basic flow pattern is indicated in the legend (e.g. A-jump, Wave) including the oscillatory flow patterns (i.e. B-wave and A-wave). The dominant oscillating phenomena were found to be, at an abrupt drop, the B-wave and A-wave flow patterns: i.e., quasi-periodical changes of B-jump and Wave flow (or A-jump and Wave flow).

A comparison between each diagram show the influence of the ratio s/y_1 on the general trend. For a given group (i.e. range of parameter s/y_1), the relationship y_1/y_t versus F_1 is basically independent of the step height. In Figs. 5 to 15 the mean absolute error of y_t/y_1 ratio is ±0.1. Figures 5 to 10 show also the classical Bélanger equation (1828) and the equation of Leutheusser and Kharta (1972) for free hydraulic jumps with fully developed inflow conditions. In the present study, the values of y_1 measured in the limited jump cases were recorded at the time-averaged position of the jump toes downstream of the abrupt drop. It is therefore reasonable to compare the experimental results of the limited jumps with the equations of Bélanger (1828) and Leutheusser and Kharta (1972) when s/y_1 is relatively small and the splashing effects are not relevant.

Figures 7 and 8 show also the regime chart of Moore and Morgan (1959) for s/y_1 equal to 2, in order to show that the results proposed in literature are well fitted by the present experimental data.

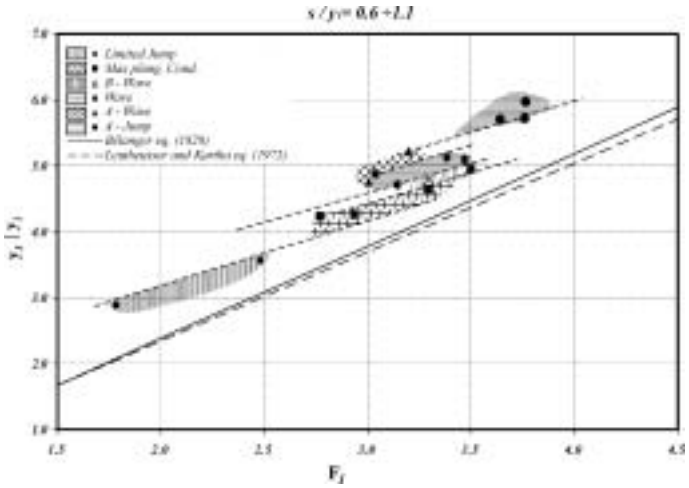

Fig. 5 Regime chart for flow configurations with $0.6 < s/y_1 < 1.1$.

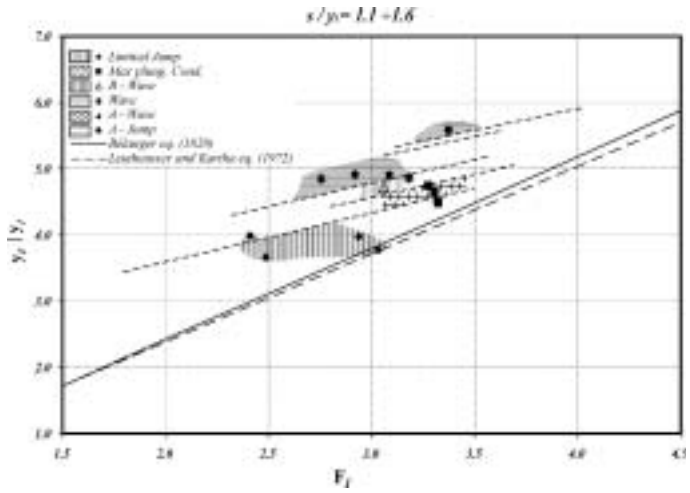

Fig. 6 Regime chart for flow configurations with $1.1 < s/y_1 < 1.6$.

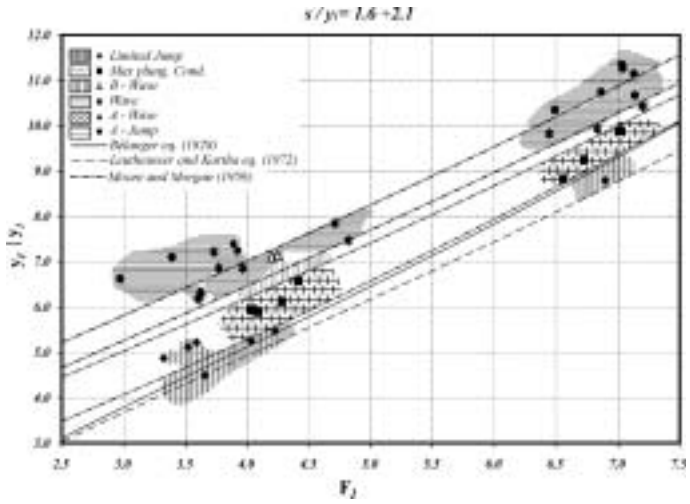

Fig. 7 Regime chart for flow configurations with $1.6 < s/y_1 < 2.1$.

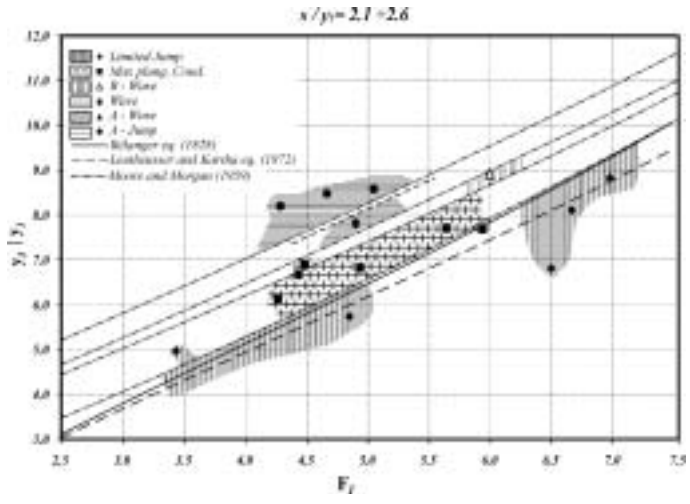

Fig. 8 Regime chart for flow configurations with $2.1 < s/y_1 < 2.6$.

Discussion

For small dimensionless drop heights ($s/y_1 < 4.1$), experimental results of limited jumps are in fair agreement with the work of Leutheusser and Kharta (1972) (Figs. 8-10). For $s/y_1 > 4.1$, the splashing effect on the flow field becomes significant and the

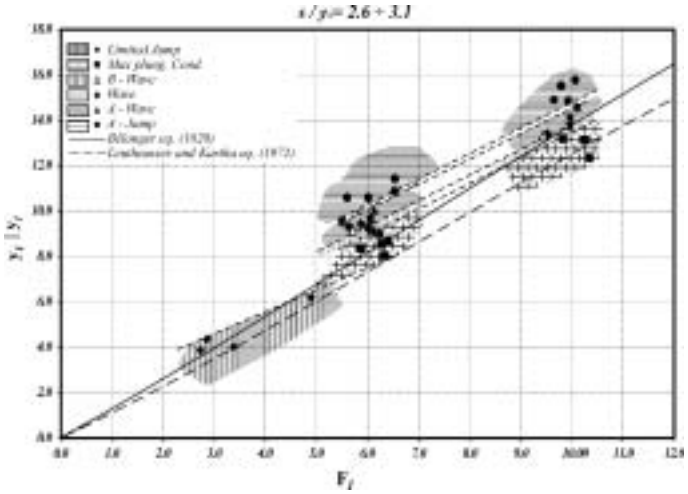

Fig. 9 Regime chart for flow configurations with $2.6 < s/y_1 < 3.1$.

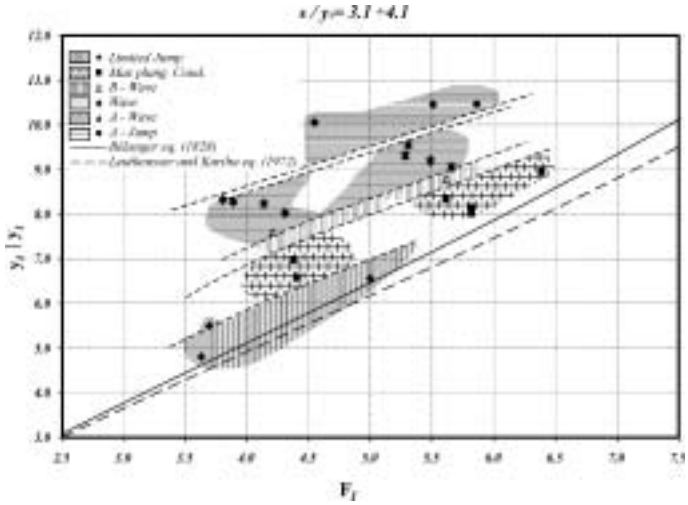

Fig. 10 Regime chart for flow configurations with $3.1 < s/y_1 < 4.1$.

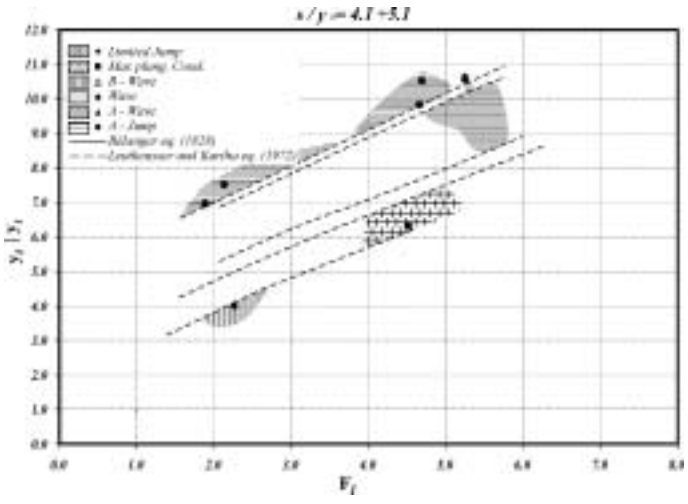

Fig. 11 Regime chart for flow configurations with $4.1 < s/y_1 < 5.1$.

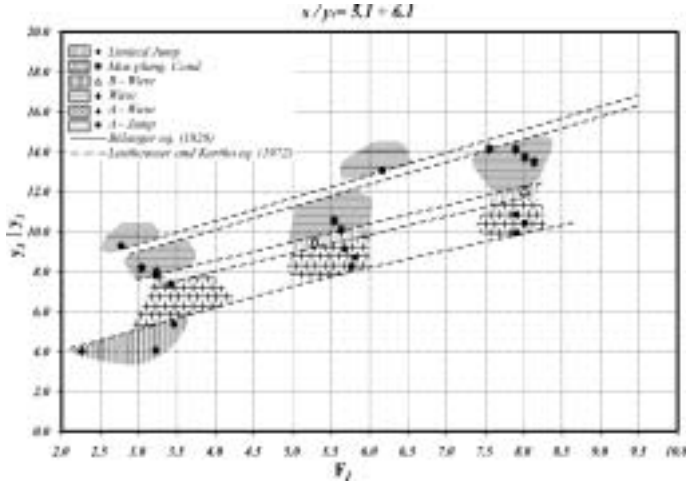

Fig. 12 Regime chart for flow configurations with $5.1 < s/y_1 < 6.1$.

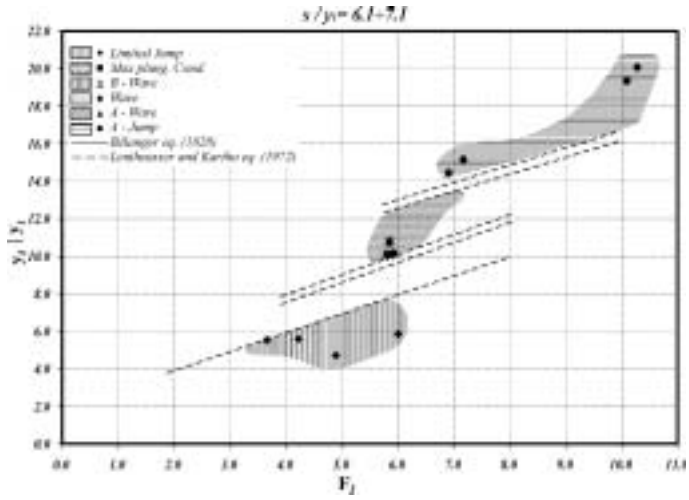

Fig. 13 Regime chart for flow configurations with $6.1 < s/y_1 < 7.1$.

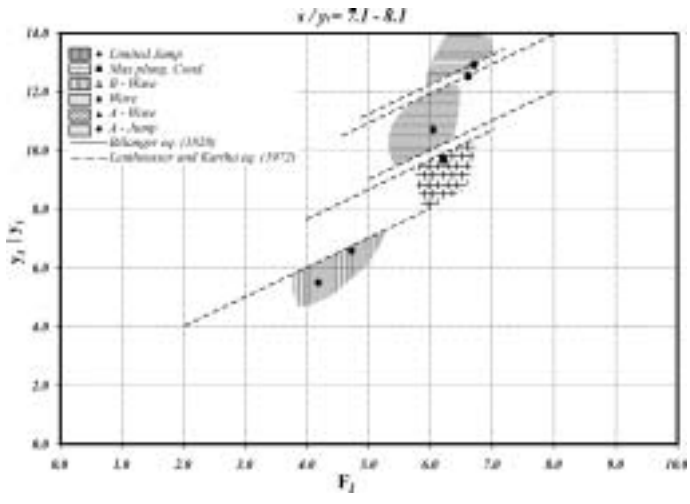

Fig. 14 Regime chart for flow configurations with $7.1 < s/y_1 < 8.1$.

equation of Leutheusser and Kharta (1972) is no longer valid. Figures 5 to 15 show that, for each bordering region between two flow patterns, the tailwater depth ratio y_t / y_1 increases with increasing step ratio s/y_1 for a fixed inflow Froude number. Previous studies generally do not provide experimental results on oscillating phenomena, i.e. quasi-periodically repeated flow conditions. It is worthwhile to observe that the quasi-periodically repeated flow configurations are generally not macroscopically visible in the cases of mean and high drop configurations, i.e. when

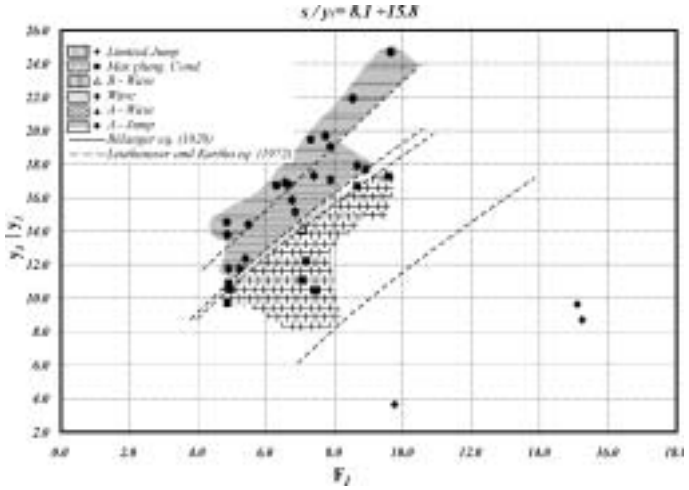

Fig. 15 Regime chart for flow configurations with $8.1 < s/y_1 < 15.8$.

$s/y_1 > 7.0$-8.0.

The quasi-periodic oscillations of jump types are accompanied by drastic instantaneous changes in the pressure under the jump (e.g. Mossa 1999). Figures 16 and 17 show a part of the time series and the amplitude spectrum of the pressure deviations from the mean measured under the hydraulic jump B32 of Table 1. The pressure tap was located at a distance of 26 cm from the time-averaged position of the jump toe. From the analysis of the pressure amplitude spectrum it is clear that even the pressure fluctuations are quasi-periodic (with a pseudo-period of about 20 s) and so strongly influenced by the oscillations between the B and wave jump types. Pressure measurements have been also carried out for other configurations confirming the conclusions earlier discussed (the results are not reported for the sake of brevity). During tests also drastic instantaneous changes in the velocity components were observed during a change of jump types (for more details see Mossa and Petrillo 1997 and Mossa 1999 where LDA velocity measurements are reported). In fact, in the regions close to the roller the amplitude spectra of the velocity components are characterised by a dominant peak at a frequency equal to the cyclic oscillations in the cases of quasi-periodic oscillation of different flow types. In contrast analogous spectra obtained for flow configurations characterised by stable jump type lack these dominant peaks. All the analysed oscillating phenomena shows the same order of magnitude of the periodicity, but it has to be noticed that the experiments carried out in the present study have not given a link between the dominant frequencies of the spectra and the hydrodynamic characteristics of the jumps.

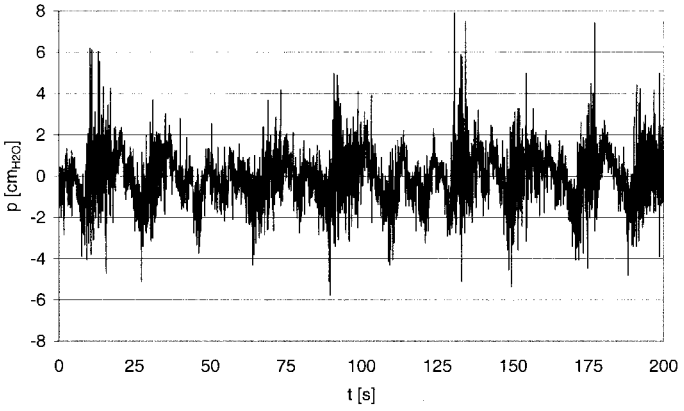

Fig. 16 Time series of the pressure deviations from the mean under hydraulic jump (configuration B32 of Table 1).

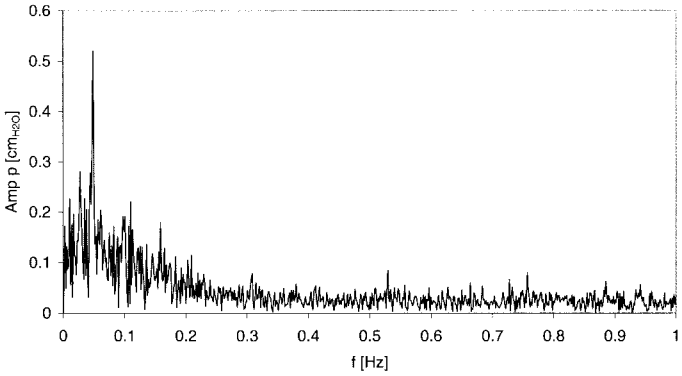

Fig. 17 Amplitude spectrum of pressure fluctuations under hydraulic jump (configuration B32 of Table 1).

Experimental results show further that the analysed configurations of limited jump are nearly independent of the s/y_1 ratio, while the other flow patterns exhibit a larger tailwater depth ratio y_t / y_1 with increasing dimensionless step height s/y_1 for a fixed inflow Froude number.

Conclusions and design recommendations

The present study reports experimental results of the transition from supercritical to subcritical flow at an abrupt drop. Such a design is practically used to stabilise the position of the jump. The experimental results show 4 to 5 basic flow patterns (Fig. 1) while the relationship between the tailwater depth ratio and the inflow Froude number may be well regrouped into eleven categories (Figs. 5 to 15): i.e., over 44 to 55 flow configurations altogether. The results highlight the different regions of flow conditions and the occurrence of oscillatory flow conditions between two different jump types characterised by quasi-periodic oscillation. These oscillations between two different jump types are responsible for the fluctuations of hydrodynamic characteristics of the motion field such as the free surface profile in the downstream region of the jump, the velocity components and pressure fluctuations within the same area. The importance of the analysis reported in the present study is also linked to design and constructive aspects of the spillway stilling basins (for further details see Chanson 1999). For design purposes, the diagrams (Figs. 5 to 15) may be used to determine the necessary drop height. It is proposed that a point (F_1-y_t / y_1) and a tentative drop height s (and, therefore, s / y_1) be first defined for conditions at maximum discharge and for the desired flow pattern. By repeating this procedure for other discharges within the expected range of discharges and for the same value of the drop height s, the designer will assess if it will be possible to prevent undesired flow conditions. This procedure might require some iterations to find an optimum value of the drop height. This analysis will highlight the different flow types due to the variations of the hydrodynamic characteristics in the

channel. It is recommended to design basins and abrupt drops taking into consideration any different flow types, with the precautionary conditions as regards the tailwater and pressure fluctuations in the channel (Sharp 1974; Armenio et al. 1997).

It is further advised to verify if, within the expected discharges, point (F_1-y_t / y_1), for the fixed value of s/y_1, it positions itself in the border between two different flow regions of the regime chart. That situation should be avoided, since it is the start of the formation of oscillating phenomena. If that is not possible, or there is a chance of variations in the hydrodynamic characteristics in the channel sufficient to start the oscillating phenomena, it is recommended that basins and abrupt drops be designed taking into consideration all the flow configurations (which will alternate in time), making reference to the worse conditions as regards the tailwater and pressure fluctuations in the channel.

References

Abdel Ghafar, A., Mossa, M. and Petrillo, A. (1995). 'Scour from flow downstream of a sluice gate after a horizontal apron', *Sixth International Symposium on River Sedimentation - Management of Sediment - Philosophy, Aims, and Techniques*, New Delhi, Editors C.V.J. Varma and A.R.G. Rao, Oxford & IBH Publishing Co. Pvt. Ltd., pp. 1069-1088.

Armenio, V., Toscano, P., Fiorotto, V. and Caroni, E. (1997). 'Effetto di un piccolo salto di fondo sulle pulsazioni di pressione al fondo di una vasca di dissipazione a risalto', *Proceedings of the Congress 'Giornate di Studio in onore del Prof. Edoardo Orabona nel centenario della nascita'*, Editoriale BIOS, Italy, pp. 111-123 (in Italian).

Armenio, V., Toscano, P. and Fiorotto, V. (2000). 'On the effects of a negative step in pressare fluctuations at the bottom of a hydraulic jump', *Journal of Hydraulic Research*, IAHR, vol. 38, no. 5, pp. 359-368.

Bélanger, J. B. (1828). 'Essai sur la Solution Numérique de quelques Problèmes Relatifs au Mouvement Permanent des Eaux Courantes' ('Essay on the Numerical Solution of Some Problems relative to Steady Flow of Water') *Carilian-Goeury*, Paris, France (in French).

Chanson, H. and Toombes, L. (1998). 'Supercritical flow at an abrupt drop: Flow patterns and aeration', *Can. Jl of Civil Eng.*, Vol. 25, No. 5, Oct., pp. 956-966.

Chanson, H. (1999). 'The hydraulics of open channel flows: an introduction', Butterworth-Heinemann, London, UK.

Chow, V. T. (1959). 'Open Channel Hydraulics', McGraw-Hill, New York, USA.

Hager, W. H. and Bretz, N. V. (1986). 'Hydraulic jumps at positive and negative steps', *Journal of Hydraulic Research*, IAHR, vol. 24, no. 4, pp. 237-252.

Hager, W. H. and Kawagoshi, N. (1990). 'Hydraulic jumps at rounded drop', *Proc. Instn Civ. Engrs*, Part 2, 89, pp. 443-470.

Hsu, E. (1950). Discussion of 'Control of the Hydraulic Jump by Sills', by Forster, J W and Skrinde, R A, *Transactions of the American Society of Civil Engineering*, Vol. 115, pp 988-991.

Leutheusser, H. J. and Kharta, V. C. (1972). 'Effects of inflow condition on hydraulic jump', *Journal of the Hydraulics Division*, ASCE, vol. 98, no. HY8, pp. 1367-1385.

Long, D., Rajaratnam, N., Steffler, P. M. and Smy, P. R. (1991). 'Structure of flow in hydraulic jumps', *Journal of Hydraulic Research*, IAHR, vol. 29, no. 2, pp. 207-218.

Moore, W. L. and Morgan, C. W. (1959). 'Hydraulic jump at an abrupt drop', *Trans. ASCE*, vol. 124, paper no. 2991, pp. 507-524.

Mossa, M. and Petrillo, A. (1997). 'Sui fenomeni alternativi in un risalto idraulico', *Proceedings of the Congress 'Giornate di Studio in onore del Prof. Edoardo Orabona nel centenario della nascita'*, Editoriale BIOS, Italy, pp. 125-153 (in Italian).

Mossa, M. and Tolve, U. (1998). 'Flow visualization in bubbly two-phase hydraulic jump', *Journal of Fluids Engineering*, ASME, vol. 120, no. 1, pp. 160-165.

Mossa, M. (1999). 'On the oscillating characteristics of hydraulic jumps', *Journal of Hydraulic Research*, IAHR, vol. 37, no.4, pp. 541-558.

Nebbia, G. (1942). 'Su taluni fenomeni alternativi in correnti libere', *L'Energia Elettrica*, fasc. I - vol. XIX, pp. 1-10.

Ohtsu, I. and Yasuda, Y. (1991). 'Transition from supercritical to subcritical flow at an abrupt drop', *Journal of Hydraulic Research*, IAHR, vol. 29, no. 3, pp. 309-328.

Rao, N. S. and Rajaratnam, N. (1963). 'The submerged hydraulic jump', ASCE *Journal of the Hydraulics Division*, Vol. 89, No HYI, pp 139-162.

Sharp, J. J. (1974). 'Observations on hydraulic jumps at rounded step', *Journal of the Hydraulics Division*, ASCE, vol. 100, no. HY6, pp. 787-795.

Notations

F_1 = inflow Froude number;
g = gravity acceleration;
P_1 = total pressure at section *1*;
P_s = total pressure on the face of the drop;
P_t = total pressure at section *t*;
q = discharge per unit width;
Re = Reynolds number ($V_1y_1 / \nu = V_ty_t / \nu$);
s = step height;
V_1 = average velocity at section *1*;
V_t = average velocity at section *t*;
We = Weber number;
y_1 = upstream water depth (water depth at section *1*);
y_t = tailwater depth (water depth at section *t*);
ε = channel roughness; and
γ = specific weight of the water.